# Elementary Steps in the Formation of Hydrocarbons from Surface Methoxy Groups in HZSM‑5 Seen by Synchrotron Infrared Microspectroscopy

ABSTRACT: Synchrotron infrared microspectroscopy has identified with high temporal resolution (down to 0.25 s) the initial events occurring when methanol vapor is in contact with a crystal of zeolite HZSM-5. The first alkenes are generated directly from methoxy groups formed at the acid sites via their deprotonation. These alkenes can either desorb directly or oligomerize and cyclize to form dimethylcyclopentenyl cations. The oligomeric and dimethylcyclopentenyl cations are the first major components of the hydrocarbon pool that precede aromatic hydrocarbons and lead to indirect alkene formation. The technique observes these events in real time.

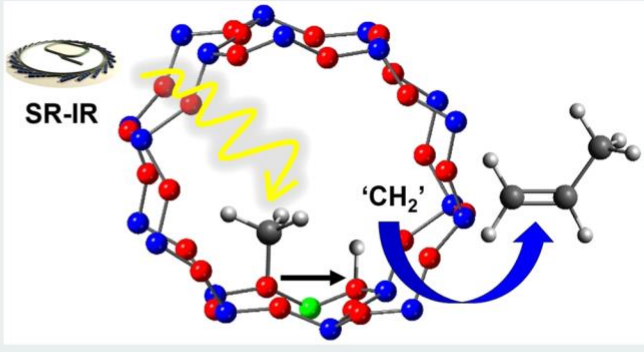


KEYWORDS: synchrotron infrared microspectroscopy, micro-FTIR, ZSM-5, methanol-to-hydrocarbons, hydrocarbon pool, carbon−carbon bond formation

The methanol-to-hydrocarbon (MTH) process was first commercialized in the 1980s with an initial emphasis on gasoline production over a ZSM-5 zeolite catalyst.[1] More recent developments have emphasized alkene production from methanol, either over ZSM-5[2] or SAPO-34 zeolites.[3,4] The mechanisms of hydrocarbon formation over HZSM-5 and other zeotypes have been widely investigated. Two recent reviews summarize the different theories which have been proposed.[5,6] It is now widely accepted that under steady state working conditions, alkenes and aromatic hydrocarbons are produced from a "hydrocarbon pool" within the zeolite pores, comprising a mixture of cyclic alkene and aromatic hydrocarbons from which reaction products are cracked and/or desorbed. It is less well understood how the hydrocarbon pool is formed in the first instance and in particular how the first carbon−carbon bonds are formed from a reactant which contains only carbon−oxygen bonds.

The first step in carbon− carbon bond formation is generally agreed to involve reaction of methanol with the Brønsted acid hydroxyl groups in the zeolite to form surface methoxy groups and eliminate water. The surface methoxy groups are key intermediates in the subsequent catalysis. Ono and Mori[7] first showed evidence for methoxy group formation in HZSM-5 from infrared spectroscopy using $CD_3OH$. Early operando infrared spectroscopic measurements reported by Forester et al. showed that both methanol and dimethyl ether vapor contacting HZSM-5 at reaction temperatures generated surface methoxy groups which were active methylating agents.[8,9] Evidence for formation of methoxy groups even at room temperature has been presented recently.[10,11] NMR evidence for these active methoxy groups has also been reported. In particular, Wang et al.[12] used a stopped flow NMR technique to isolate methoxy groups and showed that they could methylate a range of different molecules (thus forming carbon−carbon bonds). These authors also demonstrated that in the absence of other reacting species, the methoxy groups could generate alkenes directly.

Once methoxy groups are formed, several different pathways to carbon−carbon bond formation have been suggested, with varying degrees of experimental support.[5,6] For example,

methylation of dimethyl ether by methoxy groups to form the trimethyloxonium cation (which can undergo a subsequent rearrangement to form methylethyl ether),[13] hydride abstraction from methanol by the methoxy groups to form methane and formaldehyde,[14,15] an equivalent pathway involving methoxymethyl cations[16] or the recently proposed carbonylation of methoxy groups by carbon monoxide (generated from methanol decomposition) to form methyl acetate as the first carbon−carbon bond containing species.[17,18] Yamazaki et al. have presented infrared evidence for the formation of propene by direct reaction of surface methoxy groups with dimethyl ether over HZSM-5,[19] and two-dimensional NMR spectroscopy has revealed correlations between surface methoxy groups and adsorbed methanol in HSAPO-34, a smaller pore zeolite, suggestive also of direct reaction between the methoxy groups and methanol.[20,21]

Conventional spectroscopy of zeolite catalysts (transmission or diffuse reflectance infrared and NMR) inevitably report spectra integrated over many crystals in the sample. These macroscopic sampling techniques cannot respond quickly to rapid changes in local concentrations of reactants under operando conditions. The use of synchrotron infrared microspectroscopy to obtain high quality infrared spectra from large individual crystals of HZSM-5 catalysts was first reported by Stavitski et al.[22] This and subsequent work has exploited the spatial resolution of the technique down to 3−5 μm.[23,24] We report here achieving high temporal resolution, facilitated by the enhanced brightness of a synchrotron source, to perform operando infrared microspectroscopy on a time scale as short as 0.25 s on individual crystals of HZSM-5. When coupled with simultaneous mass spectral (MS) analysis of desorbed products, the operando infrared microspectroscopy (OIMS) technique identifies the initial steps of formation of the hydrocarbon pool in HZSM-5.

An induction period in the formation of alkenes, when HZSM-5 is first exposed to methanol at reaction temperatures, is well-known.[1] The measurements reported here on individual crystals show that the induction period does not arise from the conversion of methanol to dimethyl ether at 573 K but rather from a subsequent reaction step that involves the loss of the methoxy groups, regeneration of acid sites, and the subsequent generation of oligomeric hydrocarbon. The oligomer containing carbon−carbon bonds is subsequently converted to a cyclic dimethylcyclopentenyl cation. These two species are the first components of the hydrocarbon pool.

Full details of the preparation and characterization of large HZSM-5 crystals via a modified literature method, evaluation of their performance in a conventional catalytic microreactor, and the configuration of the infrared microspectrocopy experiment are given in the Supporting Information. Batches of crystals with different uniform size distributions were prepared and studied. Here are reported measurements on HZSM-5 crystals typically 150 × 60 × 60 $\mu m^3$ in size, using microscope apertures of 15 × 15 $\mu m^2$. The effects of crystal size will be reported in more detail elsewhere.[25]

Figure 1 shows the reactivity of methanol over a HZSM-5 crystal at 573 K (spectra recorded at 2 s intervals with an 8 μL pulse and at 0.25 s intervals with a 4 μL pulses). Following injection of the 8 μL pulse of methanol (Figure 1a), the zeolite Brønsted ν(OH) band at 3600 $cm^{-1}$ decreases within 60 s to 30% of its original intensity. The MS analysis of gases evolved from the Linkam cell (Figure 1b) shows the formation of dimethyl ether (m/z = 45) within several seconds of methanol

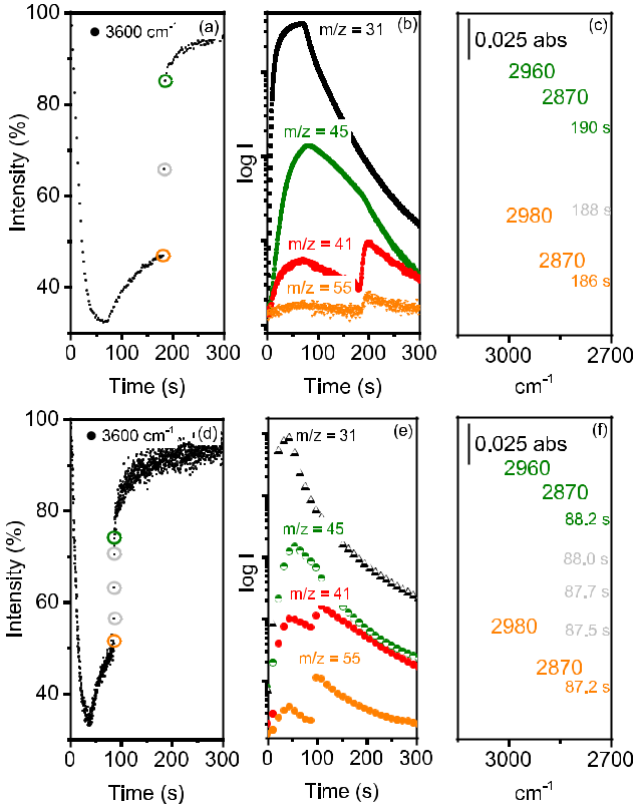


Figure 1. (a) Time course of the ν(OH) 3600 $cm^{-1}$ band intensity relative to an activated crystal recorded at 2 s intervals during the first 8 μL methanol pulse injected into a $N_2$ flow of 100 mL $min^{-1}$ over an HZSM-5 crystal at 573 K. (b) MS traces recorded during this experiment: m/z = 31 measures methanol, m/z = 45 DME, m/z = 41 propene (with a contribution from DME fragmentation), and m/z = 55 butene. (c) Evolution of the CH stretching region between 186 and 190 s. (d) The same experiment performed with 0.25 s time resolution during a 4 μL methanol pulse over a crystal from the same batch at 573 K and (e) the corresponding MS traces and (f) evolution of the CH stretching region between 87.2 and 88.2 s after injection.

injection. Formation of dimethyl ether from methanol is the first step in the conversion of methanol to hydrocarbons.[1] Dimethyl ether hydrogen bonds to the Brønsted acid site. A full set of spectra is presented in Figure S10 showing the characteristic ν($CH_3$) modes of hydrogen bonded dimethyl ether and the so-called ABC triplet of the strongly hydrogen bonded zeolite hydroxyl groups arising from Fermi resonance between the ν(OH) mode and the overtones of the corresponding δ and γ deformation modes.[26,27] Dimethyl ether forms via the sequential dissociation of methanol at acid sites to form methoxy groups followed by methylation of a second methanol to form dimethyl ether.[7−9,28] In the spectra shown in Figure S10, the characteristic infrared signature of surface methoxy groups in ZSM-5 in the ν(CH) region (bands at 2980 and 2870 $cm^{-1}$, due to asymmetric and symmetric $CH_3$ stretching modes, respectively[7−9,28]) is initially obscured by the overlapping bands of hydrogen-bonded dimethyl ether.

Figure 1 shows that as the dimethyl ether is desorbed from the crystal (between 60 and 180 s after injection of an 8 μL pulse of methanol), the ν(CH) bands of surface methoxy groups at 2980 and 2870 $cm^{-1}$ become visible (Figure 1c, orange trace). The loss of dimethyl ether corresponds to the gradual recovery of ~15% of the zeolite ν(OH) band. Subsequent to the complete loss of dimethyl ether, an abrupt

change occurs 188 s after injection of methanol. In this particular experiment, within 4 s the zeolite ν(OH) band suddenly recovers to ~90% of its original intensity (Figure 1a). At the same time, the ν(CH) bands of surface methoxy groups (2980 and 2870 $cm^{-1}$) are completely converted to new ν(CH) bands at 2960 and 2870 $cm^{-1}$, the latter broader than its predecessor (Figure 1c, green trace); and the MS (Figure 1b) shows simultaneous evolution of propene (m/z = 41) and butene (m/z = 55). (Note that the initial m/z = 41 peak at ~90 s in Figure 1b is due to fragmentation of dimethyl ether). To define more closely the time scale on which the abrupt spectral changes are occurring, we repeated the experiment described above on a fresh crystal using a smaller methanol pulse (4 μL) at a higher time resolution of 0.25 s (Figure 1d– f). The induction time for alkene formation was reduced to ~90 s for the 4 μL injection (cf. 188 s for the 8 μL injection experiment); nonetheless the changes occurring in the ν(CH) region were closely similar to those described above and occur within 0.5 s.

These spectral changes were reproduced when methanol was injected into crystals from different synthesis batches and when varying the selected region analyzed within an individual crystal, although the length of the induction period varies with crystal size as well as the methanol pulse size.

Figure 2 illustrates an experiment examining the reactivity of methanol-$d_3$ ($CD_3OH$) over a HZSM-5 crystal at 573 K. Similarly to the previous experiment, an initial decrease in ν(OH) 3600 $cm^{-1}$ band intensity relative to the fresh crystal was seen due to hydrogen bonding of dimethyl ether and the formation of methoxy groups ($ZOCD_3$) immediately after injection of methanol-$d_3$. Following a slow recovery of ν(OH) intensity over the subsequent ~90 s due to desorption of hydrogen bonded dimethyl ether, an abrupt loss of methoxy groups occurs at around 110 s after injection of $CD_3OH$ (Figure 2c), which coincides with the point of alkene formation and a rapid growth of a ν(OD) band at 2650 $cm^{-1}$.

A ZOD band can only arise from CD bond breaking. A weak band appears at 2750 $cm^{-1}$ at the same time as the CD bond breaks, which is assigned to the ν(OD) counterpart of the silanol groups in the parent zeolite associated with defects in the crystal.[28,29]

In the effluent gas phase Figure 2b, dimethyl ether-$d_6$ is the first product detected (m/z = 50 with contributions at m/z = 48 from fragmentation), but the growth of the ν(OD) bands correlates exactly with the MS detection of propene-$d_6$ (m/z = 48) and propene-$d_5$ (m/z = 47). (The earlier m/z = 47 peak coincident with dimethyl ether is barely above the baseline and may arise from a methanol-$d_2$ impurity as shown in Figure S11).

Spectra in the ν(CD) region are more complex than their ν(CH) counterparts, due to overlap of overtones of the CD bending modes,[30] and the frequency differences between species are less in the lower frequency range, so that it is not possible to clearly differentiate between loss of methoxy groups ($CD_3$) and of residual dimethyl ether-$d_6$. However, the formation of zeolite OD groups can only occur through CD bond breaking, which correlates closely with propene formation (early static infrared experiments by Ono and Mori also report CD bond breakage during propene formation[7]). We deduce a reaction step represented formally as $ZOCD_3 \rightarrow ZOD + \text{“}CD_2\text{”}$, i.e., the methoxy groups react further as carbene-like species to generate alkenes rather than as $CD_3$ cations.[19,28,31] The detection by MS of propene-$d_5$ also

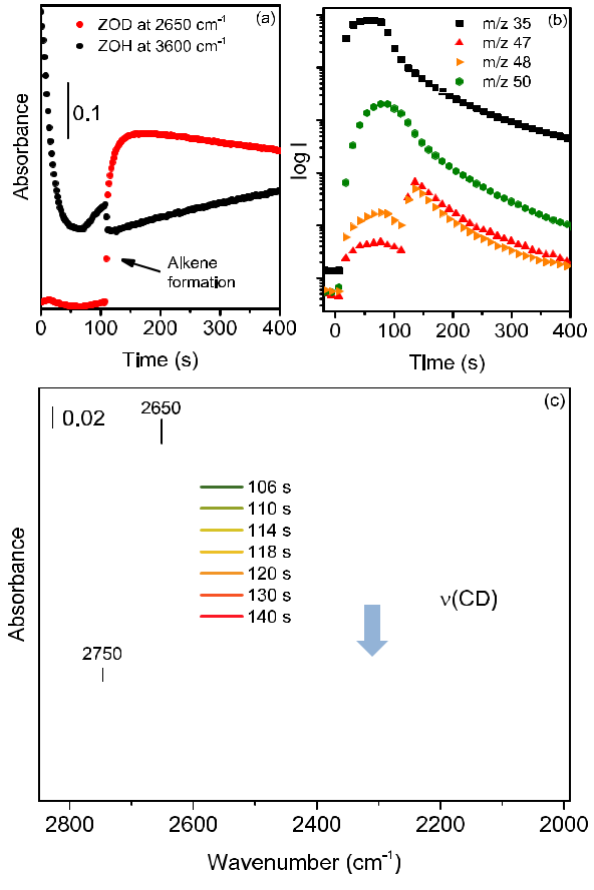


Figure 2. (a) Intensities of ν(OH) and ν(OD) bands following injection of 8 μL of $CD_3OH$ over a ZSM-5 crystal at 573 K. (b) MS analysis of evolved gases: m/z = 35 measures $CD_3OH$, m/z = 50 measures $CD_3OCD_3$, m/z = 48 measures propene-$d_6$ (with a contribution from fragmentation of $CD_3OCD_3$), and m/z = 47 measures propene-$d_5$. (c) Corresponding changes in the ν(CD) and ν(OD) regions between 106 and 140 s after injection (every second spectrum plotted for clarity).

shows that further exchange subsequently occurs with zeolite OH groups, including the silanol groups (as also seen by the change in ν(OH) intensity at this point).

Once formed, alkenes can readily oligomerize in HZSM-5 and other acid zeolites at room temperature.[32] Propene forms an oligomer in HZSM-5 which has cationic character but which can be represented as $ZO{-}CH(CH_3){-}(CH_2CH{-}(CH_3))_n{-}CH_2{-}CH(CH_3)_2$, i.e., an alkoxide species replacing the acidic hydroxyl group.[33, 34] The adsorbed species (characterized by infrared bands at 2960 and 2870 $cm^{-1}$ in the green trace of Figure 1c) is identified as an oligomeric hydrocarbon cation that is generated at the same time as loss of surface methoxy species, regeneration of Brønsted acid sites, and the generation of alkenes.

This assignment of bands to an oligomer is based on spectra obtained in a parallel experiment, when a pulse of propene was injected into $N_2$ flowing over a fresh HZSM-5 crystal at 523 K. Figure 3 shows selected spectra recorded at 2 s intervals. There is a striking similarity between the growing bands at 2960 and 2870 $cm^{-1}$ during the propene-pulse experiment (Figure 3a) and the ν(CH) profile generated after alkenes are first formed during the methanol-pulse experiments (green traces in Figure 1c,f), albeit at lower intensity and less well resolved in the case of methanol.

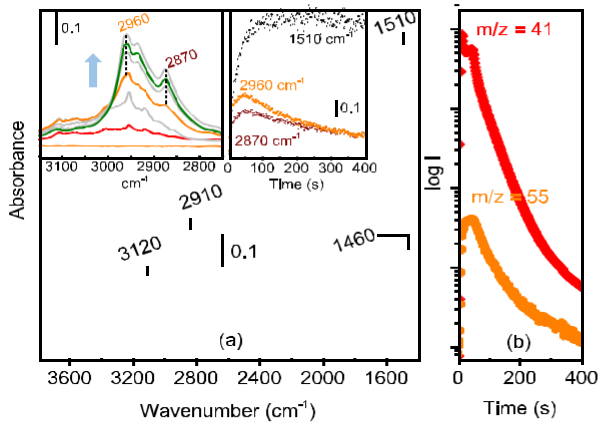


Figure 3. (a) Difference FTIR spectra recorded at 2 s intervals (first 6 scans shown) following a 2 mL propene pulse into a $N_2$ flow over an HZSM-5 crystal at 523 K. The overlaid black curve is the final spectrum in the series at 400 s after injection of propene. Insets show expansion of the CH region and a plot of intensities of the 2960, 2870, and 1510 $cm^{-1}$ bands versus time. (b) Mass spectrometer traces following injection of propene at 523 K (m/z = 41 measures propene and m/z = 55 butene).

The intensities of the oligomer bands at 2960 $cm^{-1}$ ($CH_3$ asymmetric stretching mode) and 2870 $cm^{-1}$ ($CH_3$ and $CH_2$ symmetric stretching modes) decay with time, which correlates well with the MS trace of butene (m/z = 55) evolved during the propene pulse. A secondary peak can also be seen in the m/z = 41 trace due to propene. These correlations suggest that butene and secondary propene are formed by cracking and desorption of the oligomer.

As oligomer is lost, the spectrum evolves further. In particular, bands at 1510 and 1460 $cm^{-1}$ grow in intensity and then remain constant. These bands and others at 3120 and 2910 $cm^{-1}$, which are evident in Figure 3a after the oligomer species has declined, are considered further below. Similar spectral changes were seen when ethene was injected into a fresh crystal (See Figure S13). Blank experiments showed a negligible contribution to the spectra from gas phase alkenes in the cell.

The question then arising is how the oligomer is formed in the first place. Is the oligomer formed directly from methoxy groups (2980, 2870 $cm^{-1}$) and then cracked to form the alkenes, or are the alkenes detected by MS (m/z = 41 and 55) formed directly from methoxy groups and then go on to oligomerize?

To answer this question, a temperature jump methanol-pulse experiment was performed. Figure 4 describes the reactivity of surface methoxy groups, which were generated by injecting two successive pulses of methanol over an HZSM-5 crystal at 523 K and then holding the sample at this temperature in flowing nitrogen until the hydrogen bonded dimethyl ether was completely lost, so that the spectrum showed the characteristic fingerprint of methoxy groups (Figure 4c). The OH intensity at this point (~70% of the original) suggests that ~30% of the OH groups have formed methoxy groups. Note that in this experiment, no residual bands of adsorbed dimethyl ether remain at this point. Then the temperature was raised by 5 K and the spectrum monitored versus time. After a further delay, the OH intensity suddenly recovered to ~90% of that in the fresh crystal and a burst of propene and butene was detected in the mass spectrum. No oligomer species were detected at this

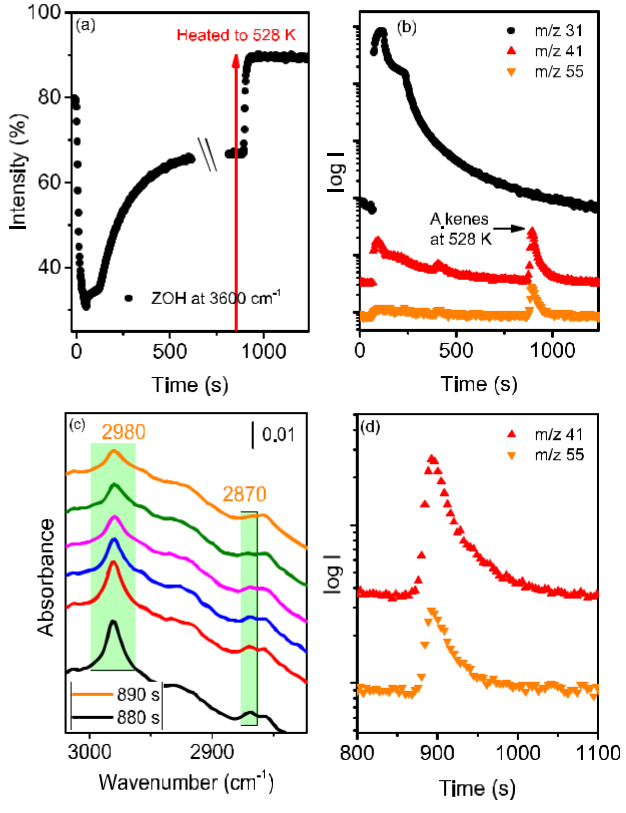


Figure 4. (a) ν(OH) intensity relative to initial fresh crystal versus time following injection of the second of two pulses of methanol over a ZSM-5 crystal at 523 K. The arrow marks the point at which the temperature was raised to 528 K. (b) Corresponding MS traces (m/z = 31 measures methanol (with a contribution from fragmentation of dimethyl ether); m/z = 41, propene (with a contribution from fragmentation of dimethyl ether), and m/z = 55, butene). (c) Spectra measured at 2 s intervals in the ν(CH) region at the point where the ν(OH) intensity increases. (d) MS traces for propene (m/z = 41) and butene (m/z = 55) during the time interval where the ν(OH) intensity increases.

temperature (528 K), which suggests that the alkenes are formed directly from the surface methoxy groups and at low concentrations can escape from the zeolite without oligome-rization, i.e., the oligomer is not formed directly from the methoxy groups but via alkenes.

The presence of a second hydrocarbon species showing bands at 3120, 2910, 1510, and 1460 $cm^{-1}$ was revealed in the propene-pulse experiment after the decay of the oligomer bands (black trace in Figure 3a). This hydrocarbon species is also evident in spectra recorded when multiple pulses of methanol were injected into an HZSM-5 crystal at 573 K. Figure 5 shows, for example, spectra measured after injection of three successive 8 μL pulses of methanol each ~300 s apart. The spectra measured at the leading edge of the third methanol pulse in Figure 5 are dominated by the bands of hydrogen bonded dimethyl ether (red trace), but as these are lost the oligomer species becomes evident (orange trace). Gradual loss of the oligomer bands reveals the second species generated from propene, which dominates the spectrum 186 s after injection of the third pulse (black trace). Also evident in the second and third pulses was an additional band at 1620 $cm^{-1}$ characteristic of methylated aromatics which was not seen in the first methanol pulse at 573 K or in the propene experiment at 523 K.

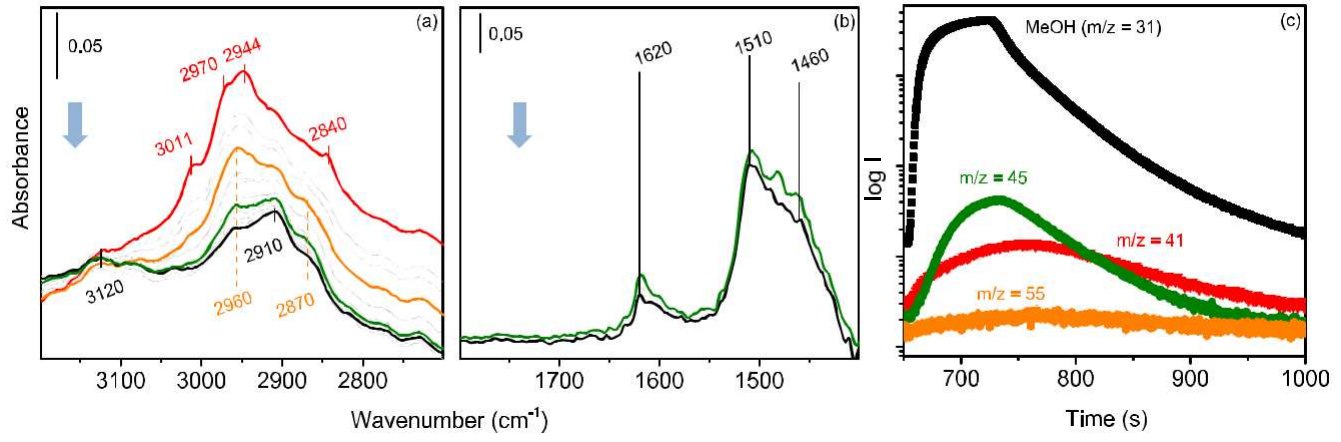


Figure 5. (a) Infrared spectra measured at 2 s intervals in (a) the ν(CH) and (b) the ν(C−C) regions following injection of a third 8 μL pulse of methanol over an HZSM-5 crystal at 573 K 650 s after the first pulse shown in Figure 1. Highlighted spectra in red, orange, green, and black at 48, 76, 128, and 186 s after the injection. (c) MS traces during the third pulse (time axis is from the first pulse): m/z = 31 measures methanol, m/z = 45 measures DME, m/z = 41 measures propene (with a contribution from DME fragmentation), and m/z = 55 measures butene.

The second species generated from propene and formed in the second and third methanol pulses exhibiting bands at 3120, 2910, 1510, and 1460 $cm^{-1}$ is identified as the 1,3-dimethylcyclopentenyl cation (DMCP). The infrared spectrum of the DMCP cation in the gas phase is known.[35] The frequencies and relative intensities of the bands seen here with propene and methanol agree well with those reported for the gas phase species. The same species was generated by reacting dimethyl ether over crystals of HZSM-5; the frequencies and relative intensities of the DMCP bands are found to be the same in different sized crystals and at different reaction temperatures, whether generated from methanol, dimethyl ether, ethene, or propene. Furthermore, the expected frequency shifts are seen when DMCP is formed from methanol-$d_4$ (see Figure S11 and Table S2).

The importance of DMCP in MTH catalysis was first demonstrated in pulse-quench NMR experiments by Haw et al., who showed that the DMCP cation was generated in less than 8 s after injection of dimethyl ether into HZSM-5 at 573 K, and its appearance in the NMR spectrum correlated with the first formation of alkene products in the gas phase.[36] The same cation was generated when HZSM-5 was exposed to ethene at 623 K, and alkene products were generated on its decomposition. At lower temperatures, long chain oligomer species were formed from ethene. More recent NMR experiments have also identified cyclopentenyl cations as well as many other related cyclic cations as important components of the hydrocarbon pool in HZSM-5,[5,6,37,38] but according to Haw et al. the 1,3-dimethylcyclopentenyl species is the first one formed (and an explanation for its particular stability in ZSM-5 has been proposed[39]).

Theoretical calculations suggest that the formation of cyclic hydrocarbons from ethene and propene occurs via oligomeric species and that 5-ring formation precedes 6-ring formation.[40] As pointed out by Haw et al., stoichiometry demands that formation of DMCP cations from oligomer requires concomitant formation of alkanes, e.g., $C_9H_{19}OZ \rightarrow C_7H_{11}OZ + 2\ CH_4$. It is possible that the methane commonly reported as an initial product of methanol conversion over ZSM-5[5,6] is formed during the cyclization step rather than through hydrogen abstraction from methanol by surface methoxy groups. Once DMCP is present in the zeolite, it may undergo methylation and skeletal rearrangement to form toluene or other methylated aromatic products through chemistry which has been well described in the literature.[5,6] The weak 1620 $cm^{-1}$ band seen in the second and third methanol pulses is assigned to toluene or related aromatic species. At higher reaction temperatures and in smaller crystals, this band has higher relative intensities, consistent with enhanced yields of methylaromatic products detected in the MS analysis (see Figure S12). A relationship between the 1620 $cm^{-1}$ band and aromatic product yields was also seen when HZSM-5 crystals were exposed to a continuous flow of dimethyl ether at higher temperatures (Figure S13).

Scheme 1 summarizes the species detected in these infrared experiments along with the infrared frequencies assigned to them. The crucial initiating step in carbon−carbon bond formation from methanol is the deprotonation of initially formed surface methoxy groups, which leads to alkene formation via carbene-like species.

The fact that alkenes are formed only after adsorbed dimethyl ether is lost suggests that this chemistry does not involve reaction of the surface methoxy groups with adsorbed dimethyl ether, as previously proposed but rather condensation of adjacent methoxy groups. The infrared spectra measured here show no evidence for formation of carboxylate groups expected from carbonylation of surface methoxy groups.[15,17,18] Figure S15 shows spectra measured from methyl acetate injected into HZSM-5 crystals at various temperatures, demonstrating the sensitivity of the technique to the presence of surface carboxylate species. We therefore believe that under the reaction conditions employed here, a mechanism for direct carbon−carbon bond formation involving formalde-hyde[14,15,41,42] or methyl acetate[17,18] is not occurring. Once alkenes are formed, they may escape the zeolite or oligomerize. The resulting oligomer can crack to provide an additional source of alkenes or cyclize to form DMCP. The oligomer and the DMCP can be regarded as the first components of the hydrocarbon pool and, as suggested by Haw et al.,[36] both act as a more efficient indirect source of alkenes (and ultimately methylaromatics) than the direct process seen in the initial stages of the reaction.

Detailed spectra and MS analyses from crystals of different sizes and at different reaction temperatures will be reported elsewhere.[25] The data presented here clearly illustrate the rapid time resolution achievable with synchrotron infrared micro-

Scheme 1. Reaction Pathways and Species Identified Spectroscopically in This Work

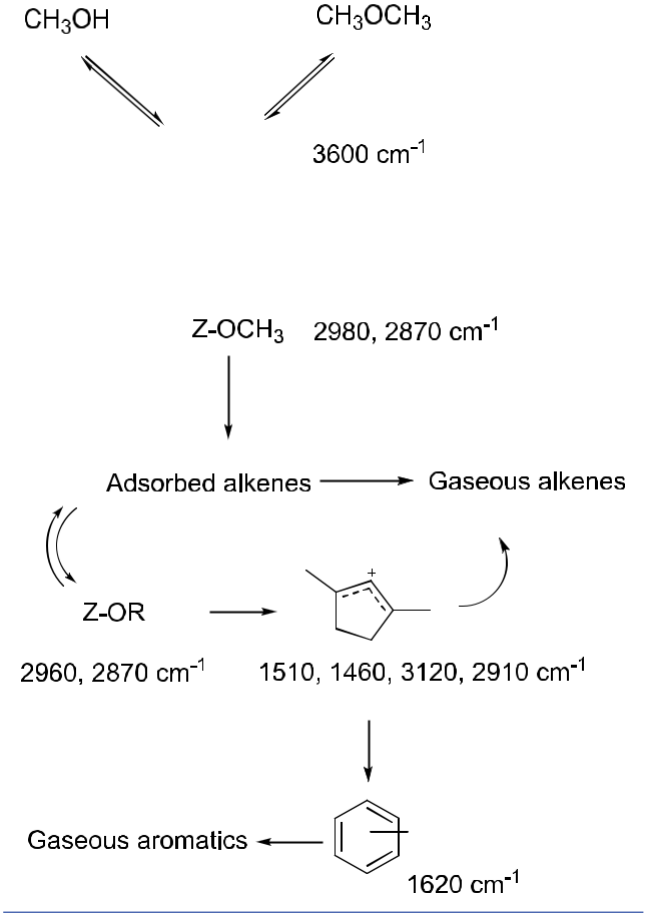


spectroscopy applied to single crystal zeolite catalysis, and we suggest that this technique should be readily applicable to many other types of zeolite-catalyzed reactions.

## ASSOCIATED CONTENT

* Supporting Information

The Supporting Information is available free of charge on the ACS Publications website at DOI: 10.1021/acscatal.9b01820.

Synthesis and characterization of HZSM-5 crystals, microreactor catalytic data, experimental procedures for synchrotron microspectroscopy measurements, and supplementary infrared spectra and MS data (PDF)

## AUTHOR INFORMATION

Corresponding Author

*E-mail: r.howe@abdn.ac.uk.

ORCID

Ivalina B. Minova: 0000-0002-1001-6861

Paul A. Wright: 0000-0002-4243-9957

Russell F. Howe: 0000-0003-2462-8962

Notes

The authors declare no competing financial interest.

## ACKNOWLEDGMENTS

I.B.M. and P.A.W. would like to thank the EPSRC and CRITICAT Centre for Doctoral Training for Financial Support (Ph.D. studentship to I.B.M., Grant EP/IO17008/1 and supplementary equipment Grant EP/L016419/1). The UK Catalysis Hub is thanked for resources and support provided via membership of the UK Catalysis Hub Consortium and funded by EPSRC (Grants EP/I038748/1, EP/I019693/1, EP/K014706/1, EP/K014668/1, EP/K014854/1, EP/K014714/1, and EP/M013219/1). We thank the Diamond Light Source for provision of beam time and support facilities at the MIRIAM beamline B22 (Experiments SM13725-1, SM16257-1, SM18680-1, and SM20906-1).

## REFERENCES

(1) Chang, C. D. Hydrocarbons from Methanol. Catal. Rev.: Sci. Eng. 1983, 25, 1−118.

(2) Koempel, H.; Liebner, W. Lurgi's Methanol-to-Propene. In Proceedings of the 8th Natural Gas Conversion Symposium, Natal, Brazil, 2007; pp 261−281.

(3) Jasper, S.; El-Halwagi, M. M. A Techno-Economic Comparison between Two Methanol-to-propene Processes. Processes 2015, 3, 684−698.

(4) Tian, P.; Wei, Y.; Ye, M.; Liu, Z. Methanol to Olefins (MTO): from Fundamentals to Commercialization. ACS Catal. 2015, 5, 1922−1938.

(5) Olsbye, U.; Svelle, S.; Lillerud, K. P.; Wei, Z. H.; Chen, Y. Y.; Li, J. F.; Wang, J. G.; Fan, W. B. The Formation and Degradation of Active Species during Methanol Conversion over Protonated Zeotype Catalysts. Chem. Soc. Rev. 2015, 44, 7155−7176.

(6) Yarulina, I.; Chowdhury, A. D.; Meirer, F.; Weckhuysen, B. M.; Gascon, J. Recent Trends and Fundamental Insights into the Methanol-to-hydrocarbons Process. Nature Catalysis 2018, 1, 398− 411.

(7) Ono, Y.; Mori, T. Mechanism of Methanol Conversion into Hydrocarbons over ZSM-5 Zeolite. J. Chem. Soc., Faraday Trans. 1 1981, 77, 2209−2221.

(8) Forester, T. R.; Wong, S. T.; Howe, R. F. In-situ FTIR of Methylating Species in ZSM-5. J. Chem. Soc., Chem. Commun. 1986, 1611−1613.

(9) Forester, T. R.; Howe, R. F. In-situ Studies of Methanol and Dimethylether in ZSM-5. J. Am. Chem. Soc. 1987, 109, 5076−5080.

(10) O'Malley, A. J.; Parker, S. F.; Chutia, A.; Farrow, M. R.; Silverwood, I. P.; Garcia-Sakai, V.; Catlow, C. R. A. Room Temperature Methoxylation in Zeolites: Insight into a Key Step of the Methanol-to-hydrocarbons Process. Chem. Commun. 2016, 52, 2897−2900.

(11) Matam, S. K.; Howe, R. F.; Thetford, A.; Catlow, C. R. A. Room Temperature Methoxylation in Zeolite H-ZSM-5: an Operando DRIFTS/Mass Spectrometric Study. Chem. Commun. 2018, 54, 12875−12878.

(12) Wang, W.; Seiler, M.; Hunger, M. Role of Surface Methoxy Species in the Conversion of Methanol to Dimethylether on Acidic Zeolites Investigated by in-situ Stopped Flow MAS NMR Spectros-copy. J. Phys. Chem. B 2001, 105, 12553−12558.

(13) Olah, G. A.; Doggweiler, H.; Felberg, J. D.; Frohlich, S.; Grdina, M. J.; Karpeles, R.; Keumi, T.; Inaba, S.; Ip, W. M.; Lammertsma, K. Onium Ylide Chemistry. 1. Bifunctional Acid-base-catalyzed Con-version of Heterosubstituted Methanes into Ethylene and Derived Hydrocarbons. The Onium Ylide Mechanism of the C1 → C2 Conversion. J. Am. Chem. Soc. 1984, 106, 2143−2149.

(14) Hutchings, G. J.; Gottschalk, F.; Hall, M. V. M.; Hunter, R. Hydrocarbon Formation from Methylating Agents over the Zeolite Catalyst ZSM-5. J. Chem. Soc., Faraday Trans. 1 1987, 83, 571−583.

(15) Liu, Y.; Kirchberger, F. M.; Muller, S.; Eder, M.; Tonigold, M.; Sanchez-Sanchez, M.; Lercher, J. A. Critical Role of Formaldehyde

During Methanol Conversion to Hydrocarbons. Nat. Commun. 2019, 10, 1462.

(16) Li, J.; Wei, Z.; Chen, Y.; Jing, B.; He, Y.; Dong, M.; Jiao, H.; Li, X.; Qin, Z.; Wang, J.; Fan, W. A Route to Form Initial Hydrocarbon Pool Species in Methanol Conversion to Olefins over Zeolites. J. Catal. 2014, 317, 277−283.

(17) Liu, Y.; Muller, S.; Berger, D.; Jelic, J.; Reuter, K.; Tonigold, M.; Sanchez-Sanchez, M.; Lercher, J. A. Formation Mechanism of the First Carbon-carbon Bond and the First Olefin in the Methanol Conversion into Hydrocarbons. Angew. Chem., Int. Ed. 2016, 55, 5723−5726.

(18) Chowdhury, A. D.; Houben, K.; Whiting, G. T.; Mokhtar, M.; Asiri, A. M.; Al-Thabaiti, S. A.; Basahel, S. N.; Baldus, M.; Weckhuysen, B. M. Initial Carbon-carbon Bond Formation during the Early Stages of the Methanol to Olefins Process Proven by Zeolite Trapped Acetate and Methylacetate. Angew. Chem., Int. Ed. 2016, 55, 15840−15845.

(19) Yamazaki, H.; Shima, H.; Imai, H.; Yokoi, T.; Tatsumi, T.; Kondo, J. N. Direct Production of Propene from Methoxy Species and Dimethylether Over H-ZSM-5. J. Phys. Chem. C 2012, 116, 24091− 24097.

(20) Van Wullen, L.; Koller, H.; Kalwei, M. Solid State Double Resonance Strategies for the Structural Characterization of Adsorbate Complexes involved in the MTG Process. Phys. Chem. Chem. Phys. 2002, 4, 1665−1674.

(21) Wu, X.; Xu, S.; Wei, Y.; Zhang, W.; Huang, J.; Xu, S.; He, Y.; Lin, S.; Sun, T.; Liu, Z. Evolution of C−C Bond Formation in the Methanol-to-olefins Process: from Direct Coupling to Autocatalysis. ACS Catal. 2018, 8, 7356−7361.

(22) Stavitski, E.; Kox, M. H. F; Swart, I.; de Groot, F. M. F.; Weckhuysen, B. M. In-situ Synchrotron-based IR Microspectroscopy to Study Catalytic Reactions in Zeolite Crystals. Angew. Chem., Int. Ed. 2008, 47, 3543−354.

(23) Stavitski, E.; Weckhuysen, B. M. Infrared and Raman Imaging of Heterogeneous Catalysts. Chem. Soc. Rev. 2010, 39, 4615−4625.

(24) Meirer, F.; Weckhuysen, B. M. Spatial and Temporal Exploration of Heterogeneous Catalysts with Synchrotron Radiation. Nature Rev. Materials 2018, 3, 324−340.

(25) Minova, I. B.; Matam, S. K.; Greenaway, A.; Suwardiyanto, A.; Catlow, C. R. A.; Frogley, M. D.; Cinque, G.; Wright, P. A.; Howe, R. F. Synchrotron Infrared Microspectroscopic Studies of Methanol Conversion over Individual Crystals of ZSM-5: Effects of Crystal Size, in preparation.

(26) Zecchina, A.; Bordiga, S.; Spoto, G.; Scarano, D.; Spano, G.; Geobaldo, F. IR Spectroscopy of Neutral and Ionic Hydrogen Bonded Complexes from Interaction of $CH_3OH$, $C_2H_5OH$, $(CH_3)_2O$, $(C_2H_5)_2O$ and $C_4H_8O$ with H-Y, H-ZSM-5 and H-mordenite: Comparison with Analogous Adducts Formed on the H-Nafion Superacidic Membrane. J. Chem. Soc., Faraday Trans. 1996, 92, 4863− 4875.

(27) Bordiga, S.; Lamberti, C.; Bonino, F.; Travert, A.; Thibault-Starzyk, F. Probing Zeolites by Vibrational Spectroscopy. Chem. Soc. Rev. 2015, 44, 7262−7341.

(28) Kondo, J. N.; Yamazaki, H.; Yokoi, T.; Tatsumi, T. Mechanisms of Reactions of Methoxy Species with Benzene and Cyclohexane Over H-ZSM-5 Zeolites. Catal. Sci. Technol. 2015, 5, 3598−3602.

(29) Yamagishi, K.; Namba, S.; Yashima, T. Defect Sites in Highly Siliceous HZSM-5 Zeolites: a Study Performed by Alumination and IR Spectroscopy. J. Phys. Chem. 1991, 95, 872−877.

(30) Falk, M.; Whalley, E. Infrared Spectra of Methanol and Deuterated Methanols in Gas, Liquid, and Solid Phases. J. Chem. Phys. 1961, 34, 1554−1568.

(31) Yamazaki, H.; Shima, H.; Imai, H.; Yokoi, T.; Tatsumi, T. N.; Kondo, J. N. Evidence for a "Carbene-like" Intermediate during the Reaction of Methoxy Species with Light Alkenes on HZSM-5. Angew. Chem., Int. Ed. 2011, 50, 1853−1856.

(32) Kiricsi, I.; Forster, H.; Tasi, G.; Nagy, J. B. Generation, Characterisation and Transformations of Unsaturated Carbenium Ions in Zeolites. Chem. Rev. 1999, 99, 2085−2114.

(33) Spoto, G.; Bordiga, S.; Ricchiardi, G.; Scarano, D.; Zecchina, A.; Borello, E. IR Study of Ethene and Propene Oligomerization on H-ZSM-5: Hydrogen-bonded Precursor Formation, Initiation and Propagation Mechanisms and Structure of the Entrapped Oligomers. J. Chem. Soc., Faraday Trans. 1994, 90, 2827−2835.

(34) Mlinar, A.; Zimmerman, P. M.; Celik, F. E.; Head-Gordon, M.; Bell, A. T. Effects of Bronsted Acid Proximity on the Oligomerization of Propene in HMFI. J. Catal. 2012, 288, 65−73.

(35) Mosley, J. D.; Young, J. W.; Agarwal, J.; Schaefer, H. F.; Schleyer, P. R.; Duncan, M. A. Structural Isomerization of the Gas-phase 2-norbornyl Cation Revealed with Infrared Spectroscopy and Computational Chemistry. Angew. Chem., Int. Ed. 2014, 53, 5888− 5891.

(36) Haw, J. F.; Nicholas, J. B.; Song, W.; Deng, F.; Wang, Z.; Xu, T.; Heneghan, C. Roles for Cyclopentenyl Cations in the Synthesis of Hydrocarbons from Methanol on Zeolite Catalyst H-ZSM-5. J. Am. Chem. Soc. 2000, 122, 4763−4775.

(37) Xiao, D.; Xu, S.; Han, X.; Bao, X.; Liu, Z.; Blanc, F. Direct Structural Identification of Carbenium Ions and Investigation of Host-Guest Interactions in the Methanol to Olefins Reaction Obtained by Multi-nuclear NMR Correlations. Chem. Sci. 2017, 8, 8309−8314.

(38) Wang, C.; Chu, Y.; Zheng, A.; Xu, J.; Wan, Q.; Gao, P.; Qi, G.; Gong, Y.; Deng, F. New Insight into the Hydrocarbon-pool Chemistry of the Methanol-to-olefins Conversion over Zeolite HZSM-5 from GCMS, Solid-state NMR Spectroscopy, and DFT Calculations. Chem. - Eur. J. 2014, 20, 12432−12443.

(39) Song, W.; Nicholas, J. B.; Haw, J. F. Acid-base Chemistry of a Carbenium Ion in a Zeolite under Equilibrium Conditions: Verification of a Theoretical Explanation of Carbenium Ion Stability. J. Am. Chem. Soc. 2001, 123, 121−129.

(40) Vandichel, M.; Lesthaeghe, D.; Van der Mynsbrugge, J.; Waroquier, M.; Van Spreybroeck, V. Assembly of Cyclic Hydrocarbons from Ethene and Propene in Acid Zeolite Catalysis to Produce Active Catalytic Sites for MTO Conversion. J. Catal. 2010, 271, 67−78.

(41) Martinez-Espin, J. S.; De Wispelaere, K.; Janssens, T. V. W.; Svelle, S.; Lillerud, K. P.; Beato, P.; Van Speybroeck, V.; Olsbye, U. Hydrogen Transfer versus Methylation: On the Genesis of Aromatics Formation in the Methanol-To-Hydrocarbons Reaction over H-ZSM-5. ACS Catal. 2017, 7, 5773−5780.

(42) Arora, S. S.; Bhan, A. The Critical Role of Methanol Pressure in Controlling its Transfer Dehydrogenation and the Corresponding Effect on Propylene to Ethylene Ratio during Methanol-to-Hydrocarbons Catalysis on H-ZSM-5. J. Catal. 2017, 356, 300−306.